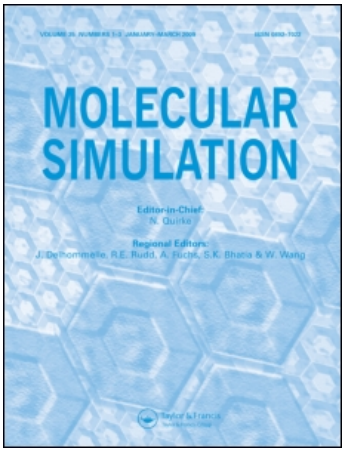

Molecular Simulation
Publication details, including instructions for authors and subscription information:
http://www.informaworld.com/smpp/title~content=t713644482

Monte Carlo simulation of the adsorption of C_2-C_7 linear alkanes in aluminophosphate $AlPO_4$-11

D. Zhang[a]; Z. Liu[a]; R. Xu[a]
[a] Department of Chemistry, Zhejiang University, Hangzhou, P. R. China

Online publication date: 27 July 2010

To cite this Article Zhang, D. , Liu, Z. and Xu, R.(2007) 'Monte Carlo simulation of the adsorption of C_2-C_7 linear alkanes in aluminophosphate $AlPO_4$-11', Molecular Simulation, 33: 15, 1247 — 1253
To link to this Article: DOI: 10.1080/08927020701697683
URL: http://dx.doi.org/10.1080/08927020701697683

Molecular Simulation, Vol. 33, No. 15, December 2007, 1247–1253

Taylor & Francis
Taylor & Francis Group

Monte Carlo simulation of the adsorption of C_2-C_7 linear alkanes in aluminophosphate $AlPO_4$-11

D. ZHANG†*, Z. LIU† and R. XU†,‡

†Department of Chemistry, Zhejiang University, Hangzhou 310027, P. R. China
‡State Key Laboratory of Inorganic Synthesis and Preparative Chemistry, College of Chemistry, Jilin University, Changchun 130012, P. R. China

(Received May 2007; in final form September 2007)

The adsorption behaviors of linear alkanes ranging in length from C_2 to C_7 in $AlPO_4$-11 have been simulated by using configurational-bias Monte Carlo technique at 313 K. The calculated heats of adsorption at zero coverage for linear alkanes, estimated by Henry coefficients, are consistent well with previously reported experimental and simulation results. The simulated isotherms for *n*-hexane in $AlPO_4$-11 at 298 K agree with the experimental data. The isotherms of C_2-C_7 linear alkane were predicted, in which butane presents a substep. The adsorbed alkane molecules are only localized in 10-membered ring channels, and adsorbed phase structures for each alkane were investigated. Total potentials for individual alkane molecule decrease with increasing number of carbon atoms. A linear change in total potential is observed for each linear alkane with increasing loading per unit cell, except that an increasing trend is found in the total potential curve of butane as the loading per unit cell is higher than two molecules.

Keywords: Simulation; CBMC; Adsorption; $AlPO_4$-11; Linear alkane

1. Introduction

$AlPO_4$-11 (AEL framework topology), a member of the aluminophosphate molecular sieves family [1], consists of one-dimensional elliptic 10-membered ring channels and has received great academic and industrial attention as catalysts, adsorbents and catalytic supports in recent years [2]. Detailed knowledge of the adsorption isotherms, adsorption location and molecular conformation of hydrocarbons in zeolites is of considerable importance for our understanding of the performance of zeolites in these applications. By using experimental measurements, however, the determination of adsorption properties of long-chain hydrocarbons can be quite time-consuming because of the slow diffusion of hydrocarbons in the pores of a zeolite [3]. Molecular simulation techniques, as a kind of "computer experiments", provide an attractive method for predicting adsorption properties of hydrocarbons in zeolites within reasonable computation time, and permit exploration at the microscopic level such as the molecular conformation and adsorption structure. The application of molecular simulation in adsorption has been allowing deepening the understanding and obtaining data that is difficult or expensive to get experimentally.

Simulations of the adsorption for long chain molecules using traditional Monte Carlo methods would require excessive computer time. To increase the fraction of successfully insertions into the sieve, the configurational-bias Monte Carlo (CBMC) technique is applied. The basic idea behind CBMC goes back many years to the work of Rosenbluth *et al.* [4]. In a CBMC simulation, chains are grown bead by bead biasing the growth process toward energetically favorable configurations, and avoiding overlap with the zeolite [5]. This makes the CBMC technique orders of magnitude more efficient than traditional Monte Carlo methods for the simulation of the adsorption of long chain molecules [6].

Aluminophosphate molecular sieves, for the unique microporous frameworks, may present different adsorption behaviors from traditional aluminosilicate molecular sieves and have received much attention in the research field of molecular simulation in recent years. The adsorption isotherms and complex adsorbed phase structures for C_1-C_5 linear alkanes in $AlPO_4$-5 have

*Corresponding author. Tel.: + 86-571-87951158. Fax: + 86-571-87951895. Email: zyliu@css.zju.edu.cn

Molecular Simulation
ISSN 0892-7022 print/ISSN 1029-0435 online © 2007 Taylor & Francis
http://www.tandf.co.uk/journals
DOI: 10.1080/08927020701697683

studied by Maris *et al.* [7] using CBMC technique. Maesen *et al.* [8] calculated the Henry coefficients and the adsorption enthalpies at zero coverage for C_5–C_7 linear and branched paraffins in $AlPO_4$-11 using CBMC technique, and investigated the shape selectivity of paraffins hydroconversion on the basis of the simulation results. Fox *et al.* [9] used the potential parameters for silicalite-1 to simulate the adsorption of C_6 alkanes in $AlPO_4$-5 and provided qualitative agreement with experiments in heats of adsorption and Henry coefficients, furthermore, they investigated the adsorption capacities and molecular orientation of the three types of C_6 alkanes including *n*-hexane, 2-methylpentane and cyclohexane.

In this works, CBMC simulations were used to determine the adsorption properties of linear alkanes ranging from ethane through heptane in $AlPO_4$-11 at 313 K. The heats of adsorption at zero coverage were investigated and compared with reported experimental and simulation data. In addition, the adsorption isotherms, structural analysis on the adsorbed phases and variation in potential were also studied.

2. Simulation details

2.1 The $AlPO_4$-11 structure

$AlPO_4$-11 has a unique three-dimensional structure with orthorhombic symmetry [10]. $AlPO_4$-11 belongs to the Ibm2 group ($a = 13.5336$, $b = 18.4821$, $c = 8.3703$ Å) and is built of straight one-dimensional channels of parallel to the crystallographic *c* direction with elliptical 10-membered ring of 3.9 × 6.3 Å. Microporous $AlPO_4$-11 is composed of strictly alternating AlO_4 and PO_4 tetrahedra linked together via joined oxygen atoms, which makes its framework electrically neutral. Unit cell data of $AlPO_4$-11 to perform calculation adsorbed amount in Section 3.2 was derived from Ref. [11].

2.2 Simulations

Monte Carlo simulations in the grand canonical ensemble [12], making use of the configurational-bias technique, was used in this work. The simulation box consists of 30 ($3 \times 2 \times 5$) unit cells of the $AlPO_4$-11 molecular sieve and corresponds to 12 channels. The periodic boundary was applied in three-dimensions to simulate an infinite system. The linear alkane molecules were described with a united-atom model; this means that CH_3 and CH_2 groups are considered as single interaction centers [13]. The bond length between these pseudoatoms was fixed at 1.53 Å. The bond-bending and torsion potentials are taken from Refs. [13–15], and the intermolecular interactions are described by a 12-6 Lennard-Jones potential. In this work, the cutoff radius of potential for all interactions was 13.8 Å, and the usual tail corrections were applied.

Following Kiselev *et al.* [16], the zeolite framework was assumed to be rigid, indicating that the molecular sieve structure is not altered by loading of guest molecules. Using rigid framework can effectively reduce the simulation time and provides a balance of accuracy and efficiency. Several authors have performed simulations using flexible zeolites [17–21] showing that a flexible lattice can influence diffusion properties. In addition, the rigid zeolite approximation will be less appropriate for large molecules at high loadings [22]. So it may be expected that the rigid zeolite approximation will be fit to the simulation of C_2–C_7 linear alkanes adsorption in zeolite in this work.

Table 1. Parameters of Lennard-Jones interactions used in this work.

	ε/k_B (K)	σ (Å)		ε/k_B (K)	σ (Å)
CH_3–CH_3	108.0	3.76	O–CH_3	80.0	3.60
CH_2–CH_2	56.0	3.96	O–CH_2	58.0	3.60

The interactions of the alkane with the zeolite were assumed to be dominated by dispersive forces involving mainly oxygen atoms [16,23], these interactions are also modeled with a Lennard-Jones potential. The potential parameters, taken from those of suitable for pure-silica type zeolites, were chosen so that the heats of adsorption at zero coverage and the Henry coefficients fit the available experimental data. The details are given in Section 3.1. These parameters for alkane–alkane and zeolite–alkane interactions shown in table 1 are derived from Refs. [5,24], respectively. The combining rules of the Lennard-Jones parameters are $\varepsilon_{ij} = \sqrt{\varepsilon_{ii}\varepsilon_{jj}}$ and $\sigma_{ij} = \sqrt{\sigma_{ii}\sigma_{jj}}$. This is a tried and tested method of determining the correct parameters for the simulation [25].

Total cycles at least 2×10^6 were performed and half of the cycles (i.e. 1×10^6) were used to reach equilibrium and summed up to get the system average. In a cycle, the number of trial moves is equal to the number of adsorbed molecules with a minimum of 20 trial moves per cycle. Twenty molecules of alkanes were inserted into the system in each configuration to calculate the system potential. For the case of the grand canonical simulations of the alkanes, the distribution of moves was 40% exchanges with the reservoir, 10% displacements, 10% rotations, 20% regrowths and 20% partial regrowths. The number of trial orientations in the CBMC scheme was six for all alkane molecules.

3. Simulation results and discussion

3.1 Heats of adsorption at zero coverage and Henry coefficients

To test model and parameters used in this work, the heats of adsorption at zero coverage were estimated by Henry coefficients in different temperatures, which were obtained from the low pressure sorption data. The simulated heats of adsorption at zero coverage from ethane to heptane are shown in table 2, and these values increase with the chain length of the sorbed alkanes and fall on a straight line (figure 1). The increasing trend in heats of adsorption is the

Table 2. Heats of adsorption at zero coverage of linear alkanes.

	Ethane	*Propane*	*Butane*	*Pentane*	*Hexane*	*Heptane*
Heats of adsorption (kJ/mol)	−30.0	−40.0	−49.1	−63.4	−72.3	−87.9

result of an increasing interaction between the adsorbed molecules and zeolite.

The obtained heats of adsorption were compared with reported experimental and simulation works. As shown in figure 1, the simulation results for the heats of adsorption at zero coverage are consistent well with the experimental data of Eder [26] and Jänchen [27] and also with the simulation results of Maesen *et al.* [8]. So, the model and L–J parameters are verified to reproduce Henry coefficients and the heats of adsorption at zero coverage for C_2–C_7 linear alkanes in AlPO$_4$-11. It is important to stress that the L–J parameters of the zeolite–alkane interaction used in this work are derived from those of pure-silica type zeolite [24], which have been applied to simulate the adsorption of aluminophosphate AlPO$_4$-5 with some success in some works [7,9]. This is due to the size and the polarizability of Al, P and Si atoms in zeolites are much smaller than those of O atoms, and the contribution of Al, P and Si atoms to the overall dispersion is much small [28]. Therefore, the computational model is simply a network of oxygen atoms and so it would seem plausible to use the same principle when studying other zeolites [9]. It shows that the model and parameters used in this work can well describe the adsorption behaviors of linear alkanes in AlPO$_4$-11 and in principle predict macroscopic properties like adsorption isotherms and microscopic behaviors, such as the preferred adsorption location and adsorbed structures within the pores.

The heat of adsorption, an important parameter characterizing the physicochemical properties of microporous materials, is a reflection to the adsorbate–adsorbent interaction. For example, a significant difference in the value of heats of adsorption is observed in VPI-5 with a 18-membered ring extra-large pore size of 12.1 Å and AlPO$_4$-5 with a 12-membered ring pore of 7.3 Å diameter, as well as AlPO$_4$-11, which belong to aluminophosphate with one-dimensional channels. Jänchen *et al.* [27] found that the heats of adsorption at zero coverage for ethane and *n*-hexane in the three aluminophosphate fit the following trend: AlPO$_4$-11 > AlPO$_4$-5 > VPI-5, which can be explained that the heats of adsorption on aluminophosphate molecular sieves with electrically neutral framework increase with increasing framework density and decreasing the pore size. For the same reason, in this work, the heats of adsorption at zero coverage of other linear alkanes adsorbed in AlPO$_4$-11 are higher than those of corresponding alkanes adsorbed in AlPO$_4$-5 [26] and VPI-5.

3.2 Adsorption isotherms

The simulated adsorption isotherm for *n*-hexane in AlPO$_4$-11 was compared with experimental data in Ref. [29] at 298 K. As shown in figure 2, the obtained isotherm is extremely closed to the experimental one, indicating that the model and parameters can reproduce the experimental isotherm very well. The adsorption isotherms for C_2–C_7 linear alkanes, simulated over a wide pressure range at 313 K using CBMC technique, were collected together for comparison and discussion and shown in figure 3.

The simulations for ethane and propane give similar adsorption isotherms, however, the pressure needed to start to adsorb in zeolite for propane is lower than that for ethane owing to the difference in the interaction between alkane molecules and zeolite. In addition, an equal value of maximum loading is observed in both alkanes, suggesting that they probably have similar adsorbed phases in the plateau region of isotherms. For the linear alkanes adsorbed in AlPO$_4$-11 in this work, the longer the chain of the linear alkane, the lower the pressure needed

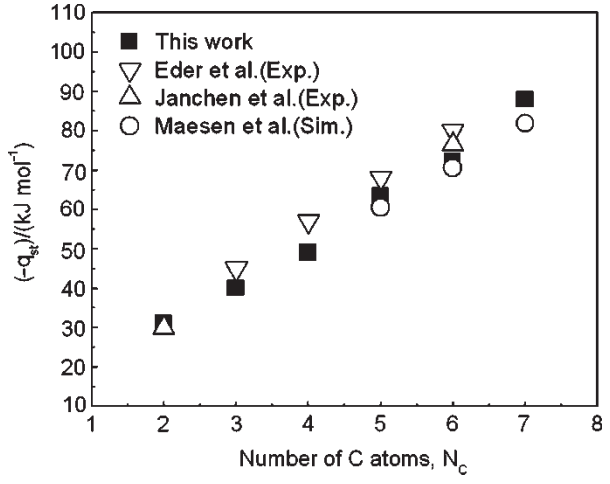

Figure 1. Heats of adsorption at zero coverage ($-q_{st}$) as a function of the number of carbon atoms (N_C) of the alkanes adsorbed in AlPO$_4$-11. The closed square symbols indicate simulation results in this work, and the open symbols indicate experimental and simulation results in other works. The experimental data are taken from Eder *et al.* [26], Jänchen *et al.* [27], the simulation data from Maesen *et al.* [8].

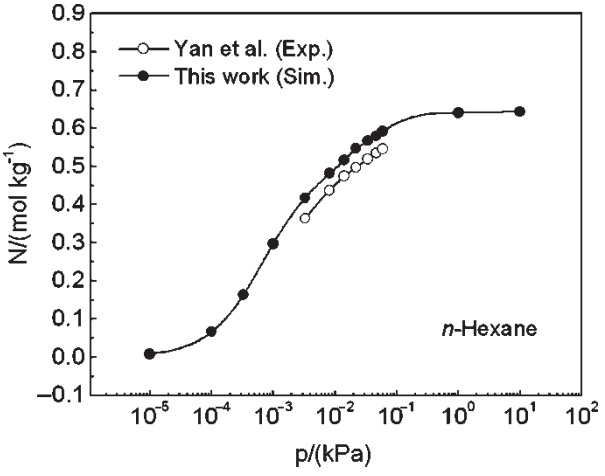

Figure 2. Comparison of simulated adsorption isotherm (the closed symbols) with experimental data (the open symbols) for *n*-hexane in AlPO$_4$-11 at 298 K. The experimental data are taken from Yan *et al.* [29].

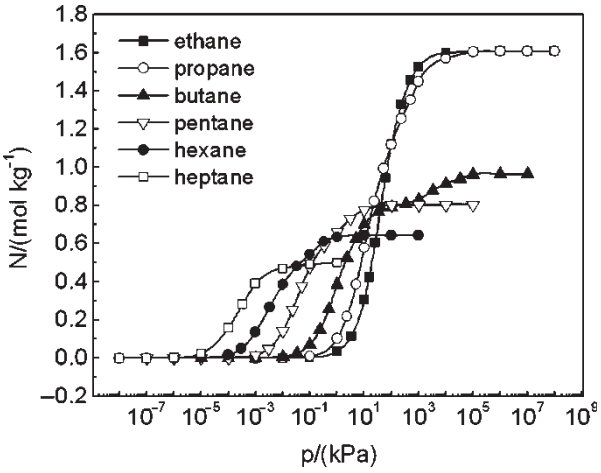

Figure 3. Simulated adsorption isotherms for C_2–C_7 linear alkanes in $AlPO_4$-11 at 313 K.

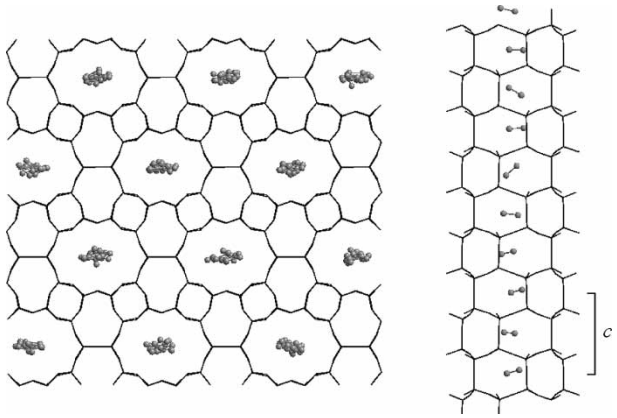

Figure 4. Snapshots of the ethane adsorbed phase at the maximum loading. The left figure is a projection of *ab* plane, the right is a projection of *ac* plane in one channel. The lines represent the zeolite framework, and the ethane molecules are represented by "ball and stick" model.

to start to adsorb in zeolite. This can be attributed to the large heat of adsorption of the long-chain alkane, which has strong affinity with zeolite framework. For the alkanes larger than butane, the maximum loading decreases with the chain length of the sorbed alkane with a decrement of approximately 0.16 mol kg^{-1} per additional CH_2 group, at the same time, the pressure needed to reach maximum loading decreases with increasing carbon number of adsorbed alkane.

The adsorption isotherm of butane shows a distinct inflection at the pressure about 300 kPa. The substep and step are found at the loading of 0.80 and 0.96 mol kg^{-1}, respectively, which correspond to two different adsorbed phases. The substep in the isotherm of butane may be attributed to a structural rearrangement of the adsorbed phase [30].

3.3 Adsorbed phase structure

3.3.1 Ethane and propane. After 2×10^6 cycles have been performed, the adsorbed phase structures at the maximum loading in isotherms at 313 K were recorded. For all investigated linear alkanes, the adsorbed molecules are only localized in 10-membered ring channels.

For ethane, as shown in figure 4, the adsorbed phase at maximum capacity corresponds to the loading of four molecules per unit cell, which is characterized by one ethane molecule located at 0 and another at *c*/2 along crystallographic *c* axis in one channel. On the basis of the projection on the *ab* plane in figure 4, the two CH_3 groups of ethane molecules are located at the long axis of the ellipse pore in the same layer. The position of 0 or *c*/2 in the crystallographic *c* axis of $AlPO_4$-11 channels is a wide region, in which the molecules or groups would be located at larger space and probably exhibit particularly higher stability than the position of *c*/4 or 3*c*/4.

The adsorbed phase for propane, as shown in figure 5, similar to that of ethane, is characterized by one molecule located at 0 and another at *c*/2 along *c* axis in one channel, and the two CH_3 groups are approximately located at the same layer, and the locations of CH_2 groups are different. As observed in ethane, the maximum loading corresponds to four propane molecules per unit cell. Therefore, the similar isotherm for ethane and propane is a faithful representation for the similar adsorbed behavior.

As to the adsorption of ethane and propane in $AlPO_4$-5 described in Ref. [7], a high-density structural transition was observed in which the adsorption increases stepwise from two to four molecules per unit cell. Ethane or propane molecules are also located at the wide region in the channel pore of $AlPO_4$-5.

3.3.2 Butane. The snapshots of the adsorbed phase structures at the substep and step in isotherm are shown in figure 6. At the substep in isotherm of butane, five molecules occupy one channel in simulation box. These butane molecules are in their *trans* conformation, and their tails (the CH_3 groups) are predominantly located at the two adjacent positions of 0 and *c*/2. With increasing pressure, another butane molecule will gradually enter this

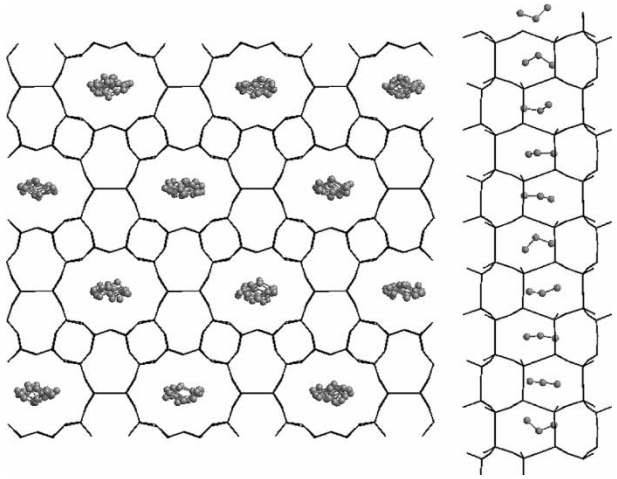

Figure 5. Snapshots of the propane adsorbed phase at the maximum loading. The left figure is a projection of *ab* plane, the right is a projection of *ac* plane in one channel.

channel. At the maximum loading, as shown in the right figure in figure 6, six butane molecules are adsorbed in one channel of simulation box. Simultaneously, we observed that four butane molecules maintain their *trans* conformation and the former adsorbed structure (one butane molecule is located in half a unit cell), the others two butane molecules marked by arrow in figure 6 are compressed into two wide regions, respectively, whose conformation is obviously different.

An analysis of the molecular conformation shows that butane molecules occupying wide regions in one channel are in the *gauche* conformation. A butane molecule in the *trans* conformation need to occupy two wide region in one channel due to the larger size. However, the main 10-membered ring pore space of $AlPO_4$-11 is sufficient to permit transition of butane molecular conformation. So at higher pressures, butane can be compressed into a wide region of one channel through *trans*–*gauche* conformation transition, which is attributed to the extent of matching in the size and shape of channel and adsorbate molecule. That is to say, the size and shape of ellipse channel in $AlPO_4$-11 nicely adapt to the conformation transition of butane molecule. However, because of the repulsion force in butane–butane and butane–zeolite, conformation transition of butane molecule cannot be observed in each wide region. The occurrence of substep in butane isotherm can be attributed to transition in the molecular conformation.

The length of substep in isotherm is relatively short, indicating that a moderate driving force is enough to compress an additional butane molecule into a channel of simulation box. Butane molecules in the *gauche* conformation would be in their higher energy conformation, which shows an increase in torsional potential and even total potential. The effect of transition in conformation on the potentials will be involved in Section 3.4. For *n*-butane adsorbed in $AlPO_4$-5 described in Ref. [7], due to the pore diameter of $AlPO_4$-5 is larger than that of $AlPO_4$-11, molecules can move freely through the entire channel and are not trapped near the adsorption sites. The whole adsorption process of *n*-butane in $AlPO_4$-5 can be considered consecutive, so no substep is observed.

As to *iso*-butane, no substep is probably observed in the isotherm. The *iso*-butane adsorption is likely to show behaviors similar to that of propane, and it would be impossible to show a conformation transition like *n*-butane.

3.3.3 Pentane, hexane and heptane. Figure 7 shows snapshots of the adsorbed phase structures for pentane, hexane and heptane in one channel at the maximum loading, respectively. For the alkanes larger than butane at the maximum loading, as shown in figure 6 (the right figure) and figure 7, the number of alkanes adsorbed in a channel decreases with the chain length with a decrement of one molecule per additional a CH_2 group. Similar to the short chain alkanes, the CH_3 and CH_2 groups are located at the long axis of the ellipse pores on the basis of a projection on the *ab* plane. For pentane, one molecule occupies half a unit cell in one channel, and their tails are apt to be located at 0 and *c*/2 (the wide region). For hexane and heptane, the tails of one molecule sometimes cannot be located at the wide region due to the confinement of chain length and conformation.

Unlike butane, after five pentane molecules are adsorbed in one channel of the simulation box, no additional molecules can be compressed into the channel at higher pressure. The size of pentane is larger than butane, indicating that the pore space is adequately occupied as a pentane molecule is adsorbed in half a unit cell. So, there is probably not enough space to load additional pentane molecules in a wide region like butane.

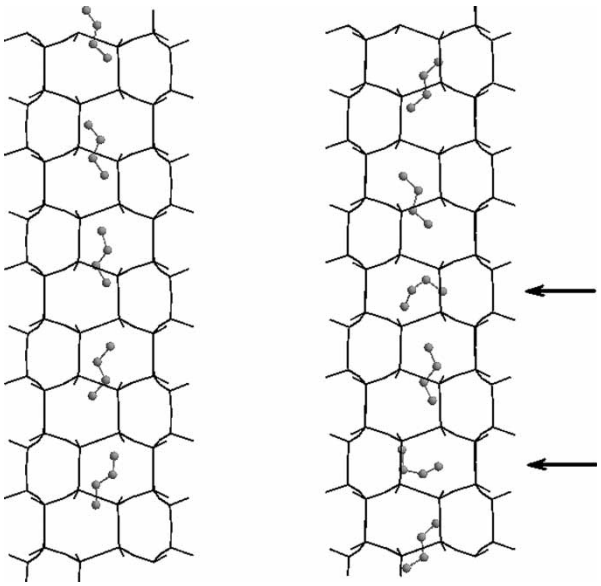

Figure 6. Snapshots of the butane adsorbed phase. The left figure is a projection of *ac* plane in one channel observed in the substep; the right figure is a projection of *ac* plane in one channel observed in the maximum loading.

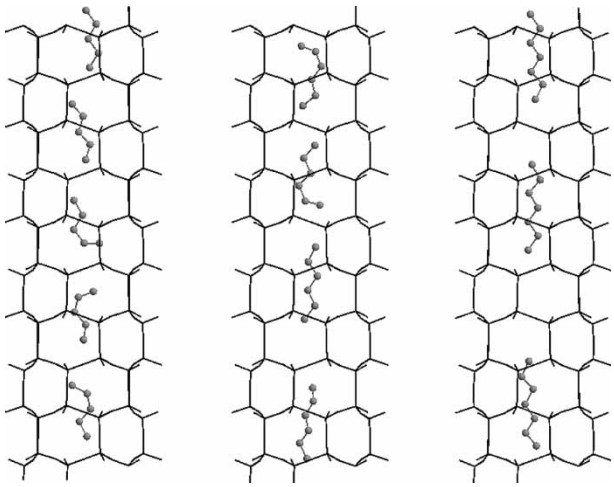

Figure 7. Snapshots of the pentane, hexane and heptane adsorbed phase at the maximum loading. The left, middle and right figure are a projections of *ac* plane in one channel for pentane, hexane and heptane, respectively.

3.4 Total potential

Total potentials for individual adsorbed alkane molecule were calculated and plotted as a function of loading per unit cell in figure 8. Total potentials decrease with increasing the carbon number of alkane adsorbed in $AlPO_4$-11, indicating that the affinity between alkane molecule and zeolite and the stability of adsorbate–adsorbent increase with increasing the chain length of the linear alkane. This is consistent well with the result that the long chain linear alkane shows a larger heat of adsorption. The interaction between nonpolar linear alkane molecules and neutral aluminophosphate $AlPO_4$-11 framework is mainly caused by van der Waals interactions. With increasing loading, the total potentials of each alkane linearly change with different slopes, except that an increasing trend is observed in the curve of butane as the loading per unit cell is higher than two molecules. For each linear alkane, as shown in figure 8, it is worth pointing out that the loading corresponded to the terminal of total potential curve is consistent with the maximum loading.

The total potential energy for ethane is the sum of intermolecular energy and external energy, and for propane is the sum of intermolecular energy, external energy and bond bending energy, respectively, moreover, for both alkanes, the value of total potential energy is absolutely dominated by external energy and the general trends with loading is mainly determined by intermolecular energy. With increasing loading, for both alkanes, the intermolecular energies linearly decrease, indicating that ethane–ethane or propane–propane intermolecular interactions are characterized by van der Waals attraction force all along, however, no remarkable change is observed in the external energies. Therefore, for both of the two alkanes, a linear decrease is observed in total potential with increasing loading, and the two total potential curves show similar slopes. The lowest total potential is observed in the adsorbed phase with four ethane or propane molecules per unit cell.

For butane, the total potential energy consists of intermolecular energy, external energy, bond bending energy and torsional energy, of which external energy is dominant one. The total potential energy and its partial energy are plotted as a function of loading per unit cell and shown in figure 9. As the loading is lower than two butane molecules per unit cell, the total potentials linearly decrease with increasing loading. The variation in torsional energy is not obvious, suggesting that the conformation of adsorbed butane molecules is in the lower energy all along. The total potential reaches the lowest value as the loading of two butane molecules per unit cell, which corresponds to the substep in isotherm. When the loading is higher than two butane molecules per unit cell, external and torsional energy are shown a remarkable increase simultaneously, which lead to an increase of the total potential. As an additional butane molecule gradually enters a channel of simulation box at an increasing pressure, the van der Waals interaction of butane–zeolite system mainly exhibits repulsion force, which leads to a sharp increase of the external potential. At the same time, for a part of butane molecules, transition from lower energy conformation (*trans* conformation) to higher energy conformation (*gauche* conformation) leads to an increase of torsional energy. In additional, the butane–butane intermolecular energy decreases all along with increasing loading, indicating that van der Waals attraction force is a determined one.

While for pentane, hexane and heptane, the total potential energy is represented to the sum of intermolecular energy, external energy, intramolecular energy, bond bending energy and torsional energy. The value of total potential energy, as observed in the former three short chain alkanes, is determined by external energy. As shown in figure 8, a similar trend is found in the total potentials of the three long chain linear alkanes, which decrease with increasing loading with more gentle slopes than that of ethane or propane. For the three long chain alkanes, with increasing loading a linear change is observed in each

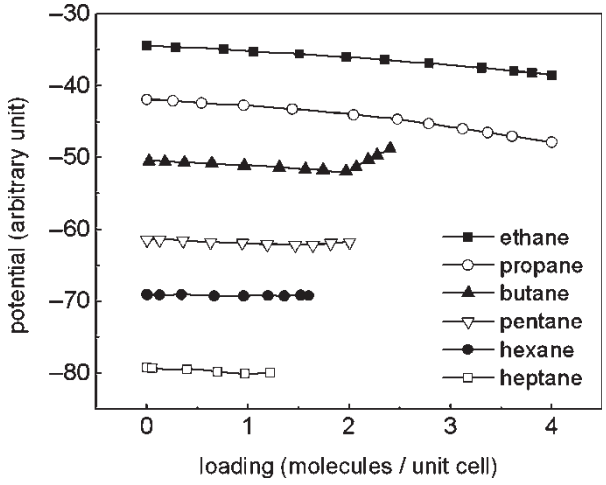

Figure 8. The total potentials for individual alkane molecule adsorbed in $AlPO_4$-11 as a function of loading per unit cell.

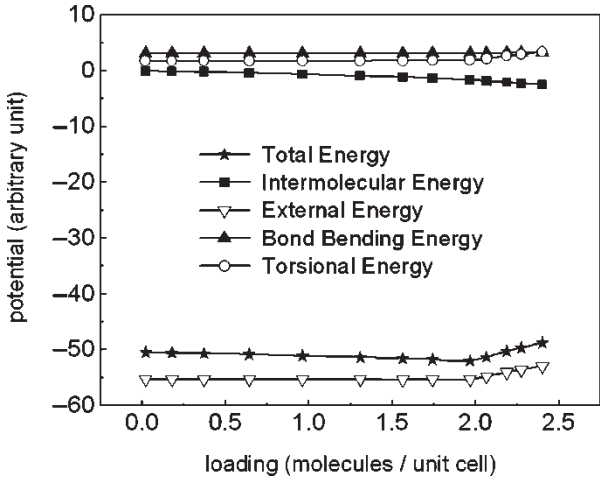

Figure 9. The total potential and partial energies for individual butane molecule adsorbed in $AlPO_4$-11 as a function of loading per unit cell.

partial energy, suggesting that the insertion of additional molecules does not have an significant effect on these partial energies.

4. Conclusions

The CBMC technique in the grand-canonical ensemble has been used for simulating the adsorption behaviors of linear alkanes ranging from ethane to heptane in $AlPO_4$-11 at 313 K. The simulated heats of adsorption at zero coverage increase with chain length, indicating that the long chain linear alkane has a larger heat of adsorption. The adsorbed linear alkane molecules are only localized in the 10-membered ring channels. Ethane and propane exhibit similar isotherm and the uniform maximum loading of four molecules per unit cell, which is characterized by the adsorbed phase with one molecule located at 0 and another at $c/2$ in one channel. An inflection is observed in isotherm of butane, in which the substep and the maximum loading correspond to the adsorbed phases that five and six butane molecules are adsorbed in one channel of simulation box, respectively. The occurrence of substep in butane isotherm can be attributed to *trans–gauche* transition in the molecular conformation. The total potential for each linear alkane maybe contains different types of partial energy, however, the external energy is dominantly one all along. The total potentials for individual alkane molecule decrease with chain length, suggesting that the affinity between the long chain alkane with zeolite is much strong. With increasing loading per unit cell, a linear change in total potential is observed for each linear alkane, except that an increasing trend is found in the total potential curve of butane as the loading per unit cell is higher than two molecules. This can be explained that some butane molecules are in a kind of *gauche* conformation with higher energy, which leads to an increase in torsional potential and even total potential.

References

[1] S.T. Wilson, B.M. Lok, E.M. Flanigen. Crystalline metallophosphate compositions. US Patent 4310440 (1982).

[2] M.E. Davis. Ordered porous materials for emerging applications. *Nature*, **417**, 813 (2002).

[3] T.J.H. Vlugt, R. Krishna, B. Smit. Molecular simulations of adsorption isotherms for linear and branched alkanes and their mixtures in silicalite. *J. Phys. Chem. B*, **103**, 1102 (1999).

[4] M.N. Rosenbluth, A.W. Rosenbluth. Monte-Carlo calculation of the average extension of molecular chains. *J. Chem. Phys.*, **23**, 356 (1955).

[5] D. Dubbeldam, S. Calero, T.J.H. Vlugt, R. Krishna, T.L.M. Maesen, B. Smit. United atom force field for alkanes in nanoporous materials. *J. Phys. Chem. B*, **108**, 12301 (2004).

[6] W.J.M. van Well, X. Cottin, B. Smit, J.H.C. van Hooff, R.A. van Santen. Chain length effects of linear alkanes in zeolite ferrierite. 2. Molecular simulations. *J. Phys. Chem. B*, **102**, 3952 (1998).

[7] T. Maris, T.J.H. Vlugt, B. Smit. Simulation of alkane adsorption in the aluminophosphate molecular sieve $AlPO_4$-5. *J. Phys. Chem. B*, **102**, 7183 (1998).

[8] T.L.M. Maesen, M. Schenk, T.J.H. Vlugt, J.P. de Jonge, B. Smit. The shape selectivity of paraffin hydroconversion on TON-, MTT-, and AEL-type sieves. *J. Catal.*, **188**, 403 (1999).

[9] J.P. Fox, V. Rooy, S.P. Bates. Simulating the adsorption of linear, branched and cyclic alkanes in silicalite-1 and $AlPO_4$-5. *Micropor. Mesopor. Mat.*, **69**, 9 (2004).

[10] J.M. Bennett, J.W. Richardson Jr., J.J. Pluth, J.V. Smith. Aluminophosphate molecular sieve $AlPO_4$-11: partial refinement from powder data using a pulsed neutron source. *Zeolites*, **7**, 160 (1987).

[11] P.S. Singh, P.N. Joshi, S.P. Mirajkar, B.S. Rao, V.P. Shiralkar. NH_3 sorption isotherms in AlPO-11 and its Si, Co, and Mn analogues. *J. Phys. Chem. B*, **103**, 5338 (1999).

[12] D. Frenkel, B. Smit. *Understanding Molecular Simulation: From Algorithms to Applications*, 2nd ed., Academic Press, New York (2001).

[13] J.P. Ryckaert, A. Bellemans. Molecular dynamics of liquid alkanes. *Faraday Discuss. Chem. Soc.*, **66**, 95 (1978).

[14] P. Van der Ploeg, H.J.C. Berendsen. Molecular dynamics simulation of a bilayer membrane. *J. Chem. Phys.*, **76**, 3271 (1982).

[15] Y. Wang, K. Hill, J.G. Harris. Confined thin films of a linear and branched octane. A comparison of the structure and solvation forces using molecular dynamics simulations. *J. Chem. Phys.*, **100**, 3276 (1994).

[16] A.G. Bezus, A.V. Kiselev, A.A. Lopatkin, P.Q.J. Du. Molecular statistical calculation of the thermodynamic adsorption characteristics of zeolites using the atom–atom approximation. *J. Chem. Soc., Faraday Trans. II*, **74**, 367 (1978).

[17] P. Demontis, G.B. Suffritti. Structure and dynamics of zeolites investigated by molecular dynamics. *Chem. Rev.*, **97**, 2845 (1997).

[18] T.J.H. Vlugt, M. Schenk. Influence of framework flexibility on the adsorption properties of hydrocarbons in the zeolite silicalite. *J. Phys. Chem. B*, **106**, 12757 (2002).

[19] A. Bouyermaouen, A. Bellemans. Molecular dynamics simulation of the diffusion of *n*-butane and *i*-butane in silicalite. *J. Chem. Phys.*, **108**, 2170 (1998).

[20] F. Jousse, D.P. Vercauteren, S.M. Auerbach. How does benzene in NaY zeolite couple to the framework vibrations? *J. Phys. Chem. B*, **104**, 8768 (2000).

[21] M. Schenk, B. Smit, T.L.M. Maesen, T.J.H. Vlugte. Molecular simulations of the adsorption of cycloalkanes in MFI-type silica. *Phys. Chem. Chem. Phys.*, **7**, 2622 (2005).

[22] J.P. Fox, S.P. Bates. Simulating the adsorption of binary and ternary mixtures of linear, branched, and cyclic alkanes in zeolites. *J. Phys. Chem. B*, **108**, 17136 (2004).

[23] A.V. Kiselev, A.A. Lopatkin, A.A. Shulga. Molecular statistical calculation of gas adsorption by silicalite. *Zeolites*, **5**, 261 (1985).

[24] T.J.H. Vlugt, W. Zhu, F. Kapteijn, J.A. Moulijn, B. Smit, R. Krishna. Adsorption of linear and branched alkanes in the zeolite silicalite-1. *J. Am. Chem. Soc.*, **120**, 5599 (1998).

[25] B. Smit, S. Karaborni, J.I. Siepmann. Computer simulations of vapour–liquid phase equilibria of *n*-alkanes. *J. Chem. Phys.*, **102**, 2126 (1995).

[26] F. Eder, J.A. Lercher. Alkane sorption on siliceous and aluminophosphate molecular sieves. A comparative study. *J. Phys. Chem.*, **100**, 16460 (1996).

[27] J. Jänchen, H. Stach, L. Uytterhoeven, W.J. Mortier. Influence of the framework density and the effective electronegativity of silica and aluminophosphate molecular sieves on the heat of adsorption of nonpolar molecules. *J. Phys. Chem.*, **100**, 12489 (1996).

[28] D. Nicholson, R.J.-M. Pellenq. Adsorption in zeolites: intermolecular interactions and computer simulation. *Adv. Colloid Interface Sci.*, **76–77**, 179 (1998).

[29] A. Yan, L. Zhou, Q. Xu. Adsorption thermodynamics of microporous aluminophosphate $AlPO_4$-11. *Acta Phys. Chim. Sin.*, **5**, 99 (1989).

[30] V. Lachet, A. Boutin, R.J.-M. Pellenq, D. Nicholson, A.H. Fuchs. Molecular simulation study of the structural rearrangement of methane adsorbed in aluminophosphate $AlPO_4$-5. *J. Phys. Chem.*, **100**, 9006 (1996).